Applied Physics Letters

Mechanical measurements on lithium phosphorous oxynitride coated silicon thin film electrodes for lithium-ion batteries during lithiation and delithiation

Cite as: Appl. Phys. Lett. **109**, 071902 (2016); https://doi.org/10.1063/1.4961234
Submitted: 20 May 2016 . Accepted: 01 August 2016 . Published Online: 17 August 2016

Ahmed Al-Obeidi, Dominik Kramer, Steven T. Boles, Reiner Mönig, and Carl V. Thompson

Mechanical measurements on lithium phosphorous oxynitride coated silicon thin film electrodes for lithium-ion batteries during lithiation and delithiation

Ahmed Al-Obeidi,[1,a)] Dominik Kramer,[2,3,b)] Steven T. Boles,[2,4,c)] Reiner Mönig,[2,3,d)] and Carl V. Thompson[1,d)]
[1]*Department of Materials Science and Engineering, Massachusetts Institute of Technology, 77 Massachusetts Avenue, Cambridge, Massachusetts 02139, USA*
[2]*Institute for Applied Materials, Karlsruhe Institute of Technology, Hermann-von-Helmholtz-Platz 1, 76344 Eggenstein-Leopoldshafen, Germany*
[3]*Helmholtz Institute Ulm for Electrochemical Energy Storage (HIU), Helmholtzstraße 11, 89081 Ulm, Germany*
[4]*Hong Kong Polytechnic University, 11 Yuk Choi Rd, Hung Hom, Hong Kong*

(Received 20 May 2016; accepted 1 August 2016; published online 17 August 2016)

The development of large stresses during lithiation and delithiation drives mechanical and chemical degradation processes (cracking and electrolyte decomposition) in thin film silicon anodes that complicate the study of normal electrochemical and mechanical processes. To reduce these effects, lithium phosphorous oxynitride (LiPON) coatings were applied to silicon thin film electrodes. Applying a LiPON coating has two purposes. First, the coating acts as a stable artificial solid electrolyte interphase. Second, it limits mechanical degradation by retaining the electrode's planar morphology during cycling. The development of stress in LiPON-coated electrodes was monitored using substrate curvature measurements. LiPON-coated electrodes displayed highly reproducible cycle-to-cycle behavior, unlike uncoated electrodes which had poorer coulombic efficiency and exhibited a continual loss in stress magnitude with continued cycling due to film fracture. The improved mechanical stability of the coated silicon electrodes allowed for a better investigation of rate effects and variations of mechanical properties during electrochemical cycling. *Published by AIP Publishing.* [http://dx.doi.org/10.1063/1.4961234]

Silicon is a promising anode material for lithium-ion batteries, offering high theoretical energy densities ($Li_{15}Si_4$: 3579 A h kg^{-1} vs. LiC_6: 372 A h kg^{-1}), low operating voltages versus lithium, and low material cost.[1] However, silicon electrodes suffer from mechanical and chemical degradation that can occur during cycling. Mechanical damage stemming from the large changes in volume (up to 300%) during lithiation and delithiation can result in electrode fracture and capacity fade.[2] Experimental investigations such as *in situ* curvature measurements provided insight into the mechanical behavior of lithiated silicon,[3–6] revealing compressive and tensile flow stresses in excess of 1 GPa and significant plastic flow during phase formation. For thin film electrodes, mechanical stresses arise due to the physical constraint imposed by the current collector/substrate interface, from lithium concentration gradients in the electrode, and from phase transformations that occur during lithium insertion and extraction.[6–8]

In addition to mechanical degradation, chemical degradation can also affect the performance of silicon anodes.[9–11] The low operating potential of silicon anodes (<0.5 V)[12] will result in reductive decomposition of the liquid electrolyte to form a surface passivating film known as solid electrolyte interphase (SEI). While a dynamically stable SEI can form on graphitic electrodes,[13–15] the SEI formed on silicon will be continually damaged during cycling due to the large volume changes of the electrode.[16–19] One strategy to address unstable SEIs and electrolyte decomposition on silicon electrodes is to use surface coatings which can function as artificial SEI layers. In solid-state thin film microbatteries, lithium phosphorous oxynitride (LiPON), a glassy lithium ion conductor, is widely used as a solid electrolyte. LiPON can be sputter deposited and is attractive due to its reasonable ionic conductivity at room temperature ($\approx 2 \times 10^{-6}$ S cm^{-1}) and wide electrochemical stability window. Electrodes coated with LiPON have been shown to have improved cyclability compared to uncoated electrodes, with LiPON serving as an artificial SEI.[8,20–23]

In this letter, the effect of LiPON coatings on stress evolution and electrolyte stability for thin film silicon electrodes is reported. LiPON coatings are found to improve the mechanical and chemical stability of silicon thin film electrodes and allow for more detailed and analytical investigations of the mechanical processes and rate dependencies during lithiation and delithiation.

Cantilevers were prepared using clean, double-side polished aluminum oxide (99.6% Al_2O_3, 254 μm thick, CoorsTek) diced into 5 mm × 16 mm pieces and were then coated with 100 nm of tungsten. Using a shadow mask, amorphous silicon (100 nm) was sputter deposited such that a 5 mm × 5 mm area remained uncoated and served as the electrical contact. For some samples, LiPON (600 nm) was deposited using reactive sputter deposition from a lithium phosphate target in the presence of nitrogen. The liquid electrolyte[10] was prepared by mixing 1,3-dioxolane (DOL, Sigma-Aldrich) and bis(trifluoromethane)sulfonimide lithium salt (Sigma Aldrich) to make a 1 M solution.

a)alobeidi@mit.edu
b)dominik.kramer@kit.edu
c)steven.t.boles@polyu.edu.hk
d)Authors to whom correspondence should be addressed. Electronic addresses: reiner.moenig@kit.edu and cthomp@mit.edu

Cantilevers were mounted in a special electrochemical cell designed for stress measurements[6,24] in which the mechanical stress was determined by tracking changes in curvature using a home-built two laser beam setup. The stresses reported are nominal stresses corresponding to the stress-thickness product divided by the initial film thickness. These nominal stress values are measured with respect to a zero stress point defined by the initial curvature of the as-prepared cantilever, so that residual stress in the as-deposited films is not accounted for. A plot of the data using a linear thickness correction as used by others can be found in the supplementary material, Figure S1. Additional information about the experimental setup as well as the effect of the LiPON layer on the curvature can be found in a previous report.[8]

Electrochemical testing began with the acquisition of cyclic voltammograms (CVs) from 1 V to 5 mV and back to 1 V at a scan rate of 50 μV s^{-1}. The first cycle CVs for both uncoated (Figure 1(a)) and LiPON-coated (Figure 1(b)) silicon electrodes reveal similar electrochemical behavior. Both show a sharp peak around 325 mV that is only observed in the first cycle. This peak is not likely to be associated with SEI formation since LiPON is an electronic insulator and cannot provide the electrons needed to drive electrolyte reduction. Possible explanations for this peak are an initial structural reorganization of the electrode or the irreversible side-reaction of lithium with oxygen in the films.[25] The strong stress response (initial compressive stress rise of ~0.5 GPa) coinciding with this sharp CV peak further suggests that this reaction occurs throughout the silicon electrode volume rather than just at the electrode interface/surface since a surface reaction is unlikely to lead to sufficiently high forces to cause the observed curvature change.[8] In the first and subsequent cycles, two prominent reversible lithiation and delithiation peaks are observed for both uncoated and LiPON-coated anodes. These peaks are consistent with those reported in the silicon anode literature.[22,26,27] No evidence of crystalline $Li_{15}Si_4$[26,28] formation is observed in either the electrochemical or mechanical data, despite having cycled below 50 mV.

While the general electrochemical behavior of uncoated and coated electrodes is similar, there are some notable differences. The first is a shift in the CV peak position. These shifts may be due to kinetic limitations arising from the finite ionic conductivity of LiPON and from the electrode and solid electrolyte interface.[29] Shifts in the CV peak position have been observed by others using LiPON-coated silicon electrodes.[30] Another difference is seen in the coulombic efficiency. For the first cycle, the coulombic efficiency of the LiPON-coated silicon electrode is 86% versus 68% for the uncoated electrode. A part of this observed capacity loss is likely due to the irreversible side reaction with oxygen in the film. From cycle two on, the average columbic efficiency of the LiPON-coated electrode rises to 98% compared to 89% for the uncoated electrode, translating to an irreversible capacity loss of about 400 mA h kg^{-1} for the uncoated electrode. A part of this capacity loss is associated with the small broad CV peak at 470 mV seen in cycles two and beyond for the uncoated electrode. This peak is likely due to the continued formation of the SEI since this peak is seen in every cycle whereas this peak is absent for the LiPON-coated electrode.

In addition to these electrochemical enhancements brought about by the LiPON coating, the mechanical behavior of the electrode is beneficially altered by the mechanical constraint imposed on the electrode surface. The effect of LiPON on electro-mechanical behavior is evident when comparing the nominal stress-capacity plots of the uncoated (Figure 1(c)) and LiPON-coated films (Figure 1(d)). While both uncoated and coated films begin with very similar

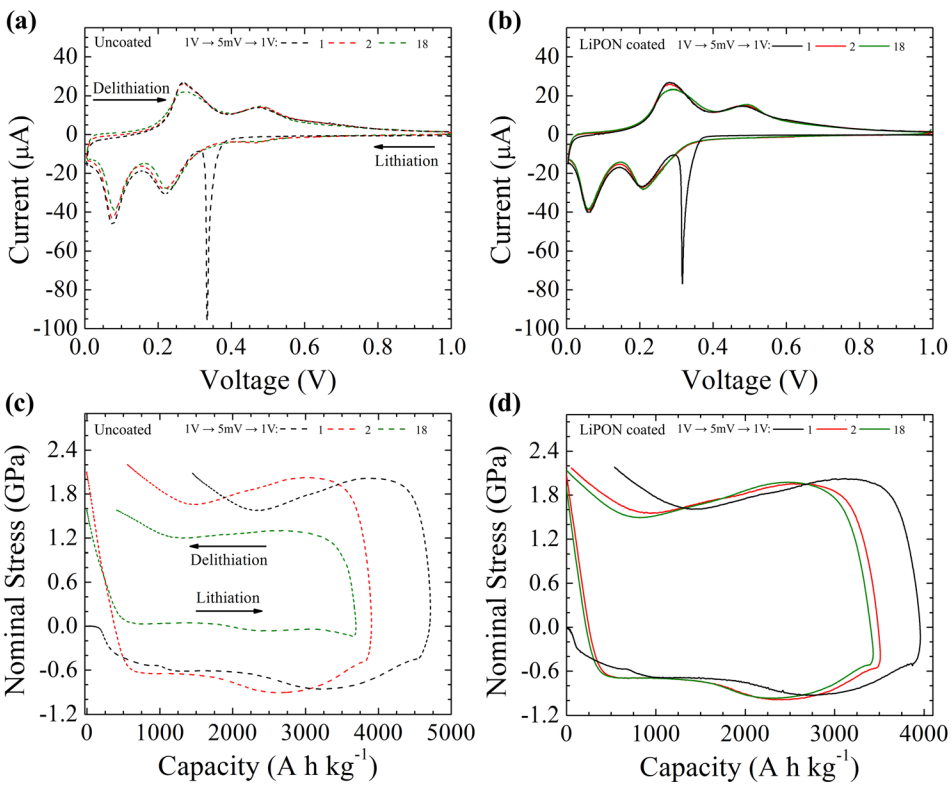

FIG. 1. Current-voltage (CV) measurements (rate: 50 μV s^{-1}) of the (a) uncoated 100-nm thick silicon electrode and the (b) LiPON-coated 100-nm silicon electrode cycled between 1 V → 5 mV → 1 V for different cycle numbers. Associated nominal stress-capacity curves for the (c) uncoated and (d) LiPON-coated silicon electrode.

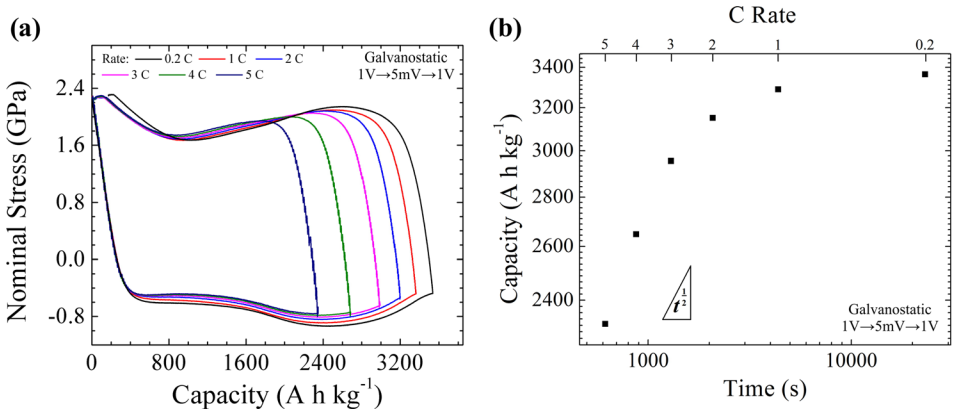

FIG. 2. (a) Nominal stress vs. capacity plots for a LiPON-coated 100-nm thick silicon film cycled galvanostatically (1 V → 5 mV → 1 V) at different rates. The C rates used are proportional to the applied currents, such that 1 C corresponds to about 65 μA cm^{-2}. At the end of delithiation, a 3 h hold was applied in order to fully delithiate the electrode. (b) Plot of the delithiation capacity as a function of delithiation time for the various cycling rates shown in (a).

nominal stress-capacity curves, the magnitude of the stress response for the uncoated film is found to decrease with continued cycling. A similar loss in stress has been previously reported for germanium electrodes and was ascribed to film fragmentation into islands.[6] In contrast to the uncoated films, LiPON-coated silicon electrodes show a stable stress response with extended cycling. LiPON seems to constrain the electrolyte/electrode surface and inhibits crack formation during delithiation, when tensile stresses are greatest.[31] This view is supported by cross-sectional SEM images (Figure S2, supplementary material) made before and after cycling that show no significant change in electrode morphology. As shown in Figure 1(d), the start of lithiation causes a rapid linear increase in nominal compressive stress. This rapid increase in stress is due to the quasi-elastic straining of the silicon film as lithium moves into interstitial sites in the amorphous silicon. The term "quasi-elastic" is used since the chemical composition of the tested material changes during the mechanical loading. This quasi-elastic straining continues until the film reaches a yield point (≈500 mA h kg^{-1}) at which quasi-plastic deformation begins. The transition from quasi-elastic to quasi-plastic behavior coincides with the emergence of the first lithiation peak. Continued lithiation causes smaller changes in nominal stress, with the emergence of a broad compressive dip at ≈1500 mA h kg^{-1}, coinciding with the second lithiation peak. The transition from lithiation to delithiation again results in a quasi-elastic linear increase in the nominal tensile stress until the film reaches the tensile yield point of Li-Si (≈3100 mA h kg^{-1}), after which quasi-plastic deformation occurs.

One main feature of the LiPON-coated electrode is that it can retain its stress profile over many cycles. This allows for stress measurements to be conducted in the absence of features associated with changes in film morphology and SEI formation.[6] The mechanical stress and the rate performance of LiPON-coated silicon were studied by galvanostatically cycling an electrode at different rates, yielding the results shown in Figure 2. As the rate of lithiation was increased, the film exhibited reduced capacity. Analysis of the electrochemical rate performance of the LiPON-coated silicon (Figure 2(b)) shows that capacity loss at high rates roughly scales with $t^{1/2}$. A similar trend has also been observed for uncoated thin film silicon electrodes[30] and for LiPON-coated germanium electrodes.[8] The reduction in capacity indicates diffusion-limited lithium transport through the film thickness. This could be either a simple diffusion limitation within a single phase or the diffusion limited motion of an interface separating regions with different stoichiometry.[8]

The stable mechanical signal of the LiPON-coated silicon electrode was further used to study the properties of individual phases present in the film during lithiation. The individual phases that form during the reaction of lithium with silicon are still not fully understood. Here, we suggest that the mechanical response of the film can be used to distinguish between different phases. Figure 3(a) shows the nominal stress-capacity behavior of a LiPON-coated silicon film cycled galvanostatically from 1 V → V_c → 1 V at a rate of 0.2 C (13 μA cm^{-2}) where V_c denominates various lithiation cutoff voltages ranging from 460 mV down to 5 mV.

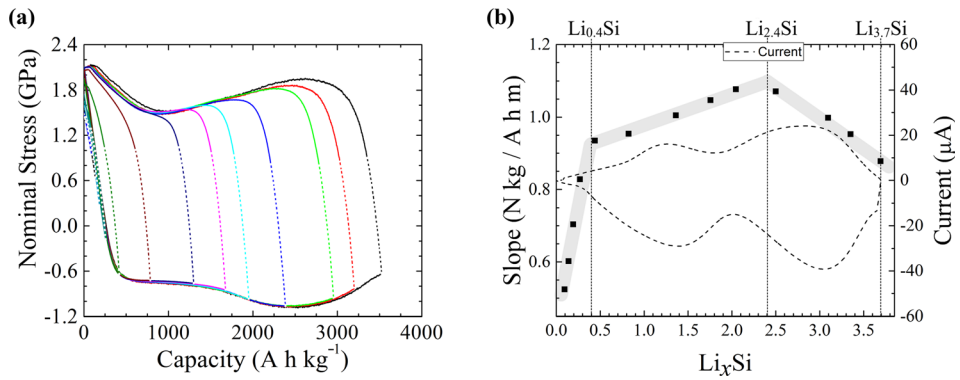

FIG. 3. (a) Nominal stress-capacity curves for a LiPON-coated 100-nm thick silicon film cycled galvanostatically from 1 V → V_c → 1 V at a rate of 0.2 C (13 μA cm^{-2}) where V_c symbolizes various lithiation cutoff voltages (460 mV, 420 mV, 380 mV, 340 mV, 300 mV, 260 mV, 220 mV, 180 mV, 140 mV, 100 mV, 70 mV, 50 mV, and 5 mV). (b) Force per charge as determined from the dotted regions in (a) as described in detail in the supplementary material. Possible Li-Si phase stoichiometries are indicated and correspond to the vertices of the three linear regions as shown in the figure.

Under galvanostatic conditions, the transition from lithiation to delithiation is driven by the change in current polarity and results in the immediate extraction of lithium from the silicon electrode surface and shrinkage in volume. This process appears as a linear, quasi-elastic tensile increase in the nominal stress-capacity plots (Figure 3(a)). The extraction of a fixed amount of lithium causes a mechanical force in the electrode (force per charge). This tensile force results from changes in the film's density and elastic modulus. Both quantities are related to the atomic configuration of the film and therefore changes in the measured force per charge may be used to distinguish between different Li_xSi-phases. Figure 3(b) shows how the force per charge varies for different cut-off voltages. The data appear to be divided into three regimes with vertices at a-$Li_{\approx 0.4}Si$, a-$Li_{\approx 2.4}Si$, and a-$Li_{\approx 3.7}Si$. Up to lithium contents of $x \approx 0.4$, lithium insertion and removal only quasi-elastically strains the silicon host structure without significant reconstruction. For concentrations beyond $x \approx 0.4$, a new amorphous phase with $x \approx 2.4$ appears to grow at the expense of the $Li_{\approx 0.4}Si$ phase, leading to a linear change in the quasi-elastic slopes with lithium content. Similarly, beyond $x \approx 2.4$, a highly lithiated amorphous phase ($x > 3.5$) appears to coexist with the a-$Li_{\approx 2.4}Si$ phase. The two coexistence ranges between these three compositions would then be responsible for the two peaks observed in the CV. Ogata *et al.*[32] propose a similar silicon delithiation sequence of a-$Li_{3.5}Si \rightarrow$ a-$Li_{2.0}Si \rightarrow$ a-Si based on *in situ* Nuclear Magnetic Resonance (NMR) data. It is important to note that the quasi-elastic relaxation curves highlighted in Figure 3(a) are not perfectly linear and that the outcome of this analysis depends on the range chosen for the linear regression. Different phases may have similar elastic moduli and the volume change per lithium may depend on the state of charge; thus, it is possible that there are phases other than those proposed above. Nevertheless, Figure 3(b) illustrates that LiPON-coated electrodes can provide mechanical data that can be used in conjunction with electrochemical measurements to investigate reaction pathways.

When silicon films are coated with LiPON, a rigid solid electrolyte, the morphological evolution observed during lithiation of uncoated films is suppressed and the evolution of mechanical stress becomes repeatable from cycle to cycle. While high mechanical stresses reversibly develop during each cycle, the capacity of the silicon electrode remains unchanged and high coulombic efficiency is retained. The repeatable behavior observed for LiPON-coated films allows for the characterization of electrochemical processes during lithiation and delithiation in films with stable planar morphology. The analysis of capacity changes during galvanostatic cycling at various rates suggests that capacities are reduced at higher rates due to diffusion limitations within the electrode. The analysis of quasi-elastic unloading curves can be used to investigate reaction pathways. The phase sequence suggested here coincides with the features in the CV and is consistent with conclusions drawn from NMR studies.

See supplementary material for a figure with converted stress data, for cross-sectional images and details on the force per charge determination.

The authors gratefully acknowledge the help of Lin Thu for assistance in sample preparation. This work was supported in part by the Low Energy Electronic Systems Program of the Singapore-MIT Alliance for Research and Technology.

[1]C.-X. Zu and H. Li, Energy Environ. Sci. **4**, 2614 (2011).
[2]L. Y. Beaulieu, K. W. Eberman, R. L. Turner, L. J. Krause, and J. R. Dahn, Electrochem. Solid-State Lett. **4**, A137 (2001).
[3]V. A. Sethuraman, M. J. Chon, M. Shimshak, V. Srinivasan, and P. R. Guduru, J. Power Sources **195**, 5062 (2010).
[4]G. Bucci, S. P. V. Nadimpalli, V. A. Sethuraman, A. F. Bower, and P. R. Guduru, J. Mech. Phys. Solids **62**, 276 (2014).
[5]V. A. Sethuraman, V. Srinivasan, A. F. Bower, and P. R. Guduru, J. Electrochem. Soc. **157**, A1253 (2010).
[6]A. Al-Obeidi, D. Kramer, C. V. Thompson, and R. Mönig, J. Power Sources **297**, 472 (2015).
[7]A. Mukhopadhyay and B. W. Sheldon, Prog. Mater. Sci. **63**, 58 (2014).
[8]A. Al-Obeidi, D. Kramer, R. Mönig, and C. V. Thompson, J. Power Sources **306**, 817 (2016).
[9]H. Wu, G. Chan, J. W. Choi, I. Ryu, Y. Yao, M. T. McDowell, S. W. Lee, A. Jackson, Y. Yang, L. Hu, and Y. Cui, Nat. Nanotechnol. **7**, 310 (2012).
[10]V. Etacheri, U. Geiger, Y. Gofer, G. A. Roberts, I. C. Stefan, R. Fasching, and D. Aurbach, Langmuir **28**, 6175 (2012).
[11]B. Philippe, R. Dedryvère, M. Gorgoi, H. Rensmo, D. Gonbeau, and K. Edström, J. Am. Chem. Soc. **135**, 9829 (2013).
[12]J. Graetz and F. Wang, in *Nanomaterials for Lithium-Ion Batteries* (Pan Stanford Publishing, 2013), pp. 69–94.
[13]P. Lu and S. J. Harris, Electrochem. Commun. **13**, 1035 (2011).
[14]S. J. Harris and P. Lu, J. Phys. Chem. C **117**, 6481 (2013).
[15]A. Tokranov, B. W. Sheldon, P. Lu, X. Xiao, and A. Mukhopadhyay, J. Electrochem. Soc. **161**, A58 (2014).
[16]L. Martin, H. Martinez, M. Ulldemolins, B. Pecquenard, and F. Le Cras, Solid State Ionics **215**, 36 (2012).
[17]S. P. V. Nadimpalli, V. A. Sethuraman, S. Dalavi, B. Lucht, M. J. Chon, V. B. Shenoy, and P. R. Guduru, J. Power Sources **215**, 145 (2012).
[18]C. Pereira-Nabais, J. Światowska, A. Chagnes, F. Ozanam, A. Gohier, P. Tran-Van, C.-S. Cojocaru, M. Cassir, and P. Marcus, Appl. Surf. Sci. **266**, 5 (2013).
[19]M. Winter, Z. Phys. Chem. **223**, 1395 (2009).
[20]X. Yu, J. B. Bates, G. E. Jellison, and F. X. Hart, J. Electrochem. Soc. **144**, 524 (1997).
[21]K. Chung, J.-G. Park, W.-S. Kim, Y.-E. Sung, and Y.-K. Choi, J. Power Sources **112**, 626 (2002).
[22]L. Baggetto, R. A. H. Niessen, F. Roozeboom, and P. H. L. Notten, Adv. Funct. Mater. **18**, 1057 (2008).
[23]J. Li, N. J. Dudney, J. Nanda, and C. Liang, ACS Appl. Mater. Interfaces **6**, 10083 (2014).
[24]Z. Choi, D. Kramer, and R. Mönig, J. Power Sources **240**, 245 (2013).
[25]H. Jung, P. K. Allan, Y.-Y. Hu, O. J. Borkiewicz, X.-L. Wang, W.-Q. Han, L.-S. Du, C. J. Pickard, P. J. Chupas, K. W. Chapman, A. J. Morris, and C. P. Grey, Chem. Mater. **27**, 1031 (2015).
[26]M. N. Obrovac and L. J. Krause, J. Electrochem. Soc. **154**, A103 (2007).
[27]J. Graetz, C. C. Ahn, R. Yazami, and B. Fultz, Electrochem. Solid-State Lett. **6**, A194 (2003).
[28]T. D. Hatchard and J. R. Dahn, J. Electrochem. Soc. **151**, A838 (2004).
[29]D. Santhanagopalan, D. Qian, T. McGilvray, Z. Wang, F. Wang, F. Camino, J. Graetz, N. Dudney, and Y. S. Meng, J. Phys. Chem. Lett. **5**, 298 (2014).
[30]J. Li, N. J. Dudney, X. Xiao, Y.-T. Cheng, C. Liang, and M. W. Verbrugge, Adv. Energy Mater. **5**, 1401627 (2015).
[31]S. P. V. Nadimpalli, V. A. Sethuraman, G. Bucci, V. Srinivasan, A. F. Bower, and P. R. Guduru, J. Electrochem. Soc. **160**, A1885 (2013).
[32]K. Ogata, E. Salager, C. J. Kerr, A. E. Fraser, C. Ducati, A. J. Morris, S. Hofmann, and C. P. Grey, Nat. Commun. **5**, 3217 (2014).